A Novel Partial Motion-decoupled 4-DOF 3T1R Parallel Mechanism with Symbolic Forward Kinematics

Huiping Shen, Zeng Fu, Guanglei Wu, Ju Li and Pengda Ye

Abstract This study proposes a novel 4-DOF parallel mechanism (PM) with three-translation and one-rotation (3T1R) motion capabilities based on the position and orientation characteristic (POC) design theory. The topological architecture of the PM is described, with detailed analysis of its topological characteristics including POC, DOF, and motion decoupling properties. Subsequently, both forward, inverse position solutions, and singularity analysis of the PM are analytically derived. The PM can balances structural rigidity with kinematic flexibility.

1 Introduction

In industrial automation and robotic manipulation, 4-DOF parallel mechanisms (PMs) with three-translation and one-rotational (3T1R) motion capabilities serve as critical enablers for precise handling and posture adjustment tasks, attracting considerable research attention in both academia and industry [1].

Kong and Gosselin developed the interesting and full motion decoupled 3-DOF Tripteron robot, and then the 4-DOF Quadrupteron robot [2].

This study presents a novel 3T1R PM with lower kinematic joints, which are developed by means of the POC design methodology [3]. Topological design and analysis, coupled with forward, inverse position solutions and singularity analysis, are illustrated.

Huiping Shen, Zeng Fu, Ju Li and Pengda Ye. Research Center for Advanced Mechanisms Theory, Changzhou University, 213164, China
Guanglei Wu. School of Mechanical Engineering, Dalian University of Technology, 116024, China

2 Topology Design and Analysis

2.1 Topology Design

To maximize payload capacity, workspace size, and to enhance rotational capability, this study develops a 4-DOF 3T1R three-limb PM composed of one hybrid branch chain I and two identical simple branch chains II and III. The hybrid branch chain I, i.e., HC I, contains two identical chains A and B (represented as P||R||R||R) that are the same with the chain in Tripteron robot[2]. While two identical simple branch chains II and III are denoted as SOC II and SOC III, respectively. Here SOC denotes single-open-chain, i.e., sequential kinematic connection comprising joints and linkages. These three distinct kinematic chains are strategically configured in parallel between the base platform 0 and the moving platform 1, as illustrated in Fig.1. This topology effectively balances structural rigidity with kinematic flexibility.

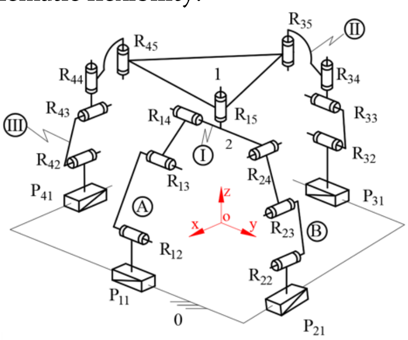

Fig. 1 A partial motion-decoupled 4-DOF 3T1R PM with symbolic forward kinematics

In Fig. 1, on the base platform 0, prismatic joints P_{11} and P_{31}, P_{21} and P_{41} maintain mutual parallelism along the Cartesian y-axis, x-axis, respectively. While prismatic joints P11 & P21 exhibit orthogonal. The moving platform 1 is linked through rotational joint R_{15} on the hybrid chain HC I, joints R_{35} on SOC II and R_{45} on the SOC III, respectively.

2.2 Topology Analysis

1) *POC analysis*

The position and orientation characteristic (POC) equations used for design of series and parallel mechanisms are respectively shown as follows[3].

$$M_{bi} = \bigcup_{i=1}^{m} M_{Ji} \tag{1}$$

$$M_{Pa} = \bigcap_{i=1}^{n} M_{bi} \tag{2}$$

where M_{Ji}—the POC set of the *i*-th joint. M_{bi}—the POC set of the end of the *i*-th branch. M_{Pa}—the POC set of the moving platform of a PM.

We define a reference point on the rotational axis R_{15} on the moving platform 1. Thus the output link 2 of the sub-PM, within the hybrid branch I, exhibits three translations (3T) . Through subsequent series integration of R_{15}, the hybrid chain I achieves composite 3T1R of end-effector motion. Then the POC sets for HC I, simple chains II and III are obtained from Eqs. (2) and (1) as follows, respectively.

$$M_{HC_{\mathrm{I}}} = \begin{bmatrix} t^3 \\ r^1(\| R_{15}) \end{bmatrix}, \quad M_{SOC_{\mathrm{II}}} = \begin{bmatrix} t^3 \\ r^2(\| \lozenge(R_{33}, R_{34}) \end{bmatrix},$$

$$M_{SOC_{\mathrm{III}}} = \begin{bmatrix} t^3 \\ r^2(\| \lozenge(R_{43}, R_{44}) \end{bmatrix}$$

Therefore, the POC set of the moving platform 1 is obtained by Eq. (2) as below.

$$M_{Pa} = M_{HC_{\mathrm{I}}} \cap M_{SOC_{\mathrm{II}}} \cap M_{SOC_{\mathrm{III}}} = \begin{bmatrix} t^3 \\ r^1(\| R_{15}) \end{bmatrix} \tag{3}$$

Eq. (3) demonstrates three-translation output and one-rotation about the R_{15} joint axis.

2) DOF calculation

According to the composition principle of PMs based on the shortest loop(S-Loop), a novel formula for the non-instantaneous degree-of-freedom (DOF) for general over-constrained and non-overconstrained PMs is given below [4].

$$F = \sum_{i=1}^{v} F_{\mathrm{j}} = F_1 + F_2 + \ldots + F_j + \ldots . + F_v \tag{4}$$

$$F_j = \sum f_{\mathrm{j}} - \xi_j \tag{5}$$

$$\xi_{Lj} = \dim.\left\{\left(\bigcap_{i=1}^{j} M_{bi}\right) \cup M_{b(i+1)}\right\} \tag{6}$$

Where

F — DOF of a PM. F_j—DOF introduced by the new j^{th} loop

v — number of independent loops ($v=m-n+1$, n—number of links, m—number of joints). ξ_j — number of independent displacement equations for the j^{th} loop

$\bigcap_{i=1}^{j} M_{bi}$ — POC sets generated by the sub-PM composed of the first j^{th} branch chain

$M_{b(j+1)}$ — POC set generated by the end link of $(j+1)^{th}$ branch chain

The PM clearly consists of three independent loops below.

(1) The first loop should be the sub-PM in hybrid chain I, namely $loop_1$\{-$P_{11}||R_{12}||R_{13}||R_{14}\perp R_{24}||R_{23}||R_{22}||P_{21}$-\}. Its number of independent displacement equation can be obtained from Eq. (6), i.e,

$$\xi_{L1} = \dim\left\{\begin{bmatrix} t^3 \\ r^1(\| R_{12}) \end{bmatrix} \cup \begin{bmatrix} t^3 \\ r^1(\| R_{22}) \end{bmatrix}\right\} = \dim\left\{\begin{bmatrix} t^3 \\ r^2(\| \lozenge(R_{12}, R_{22})) \end{bmatrix}\right\} = 5$$

Thus, the DOF of the first loop is obtained from Eq. (5), F_1=8-5=3

(2) The second loop (*i.e.*, the second sub-PM) consists of the HC_I and the simple chain II, namely $loop_2$\{-$R_{15}||R_{35}||R_{34}\perp R_{33}||R_{32}||P_{31}$-\}. From Eq. (5), we have

$$\xi_{L2} = \dim\left\{\begin{bmatrix} t^3 \\ r^1(\| R_{15}) \end{bmatrix} \cup \begin{bmatrix} t^3 \\ r^2(\| \lozenge(R_{32}, R_{34})) \end{bmatrix}\right\} = \dim\left\{\begin{bmatrix} t^3 \\ r^2(\| \lozenge(R_{32}, R_{34})) \end{bmatrix}\right\} = 5$$

Thus, the DOF of the second loop is obtained from Eq. (5), F_1=6-5=1

(3) The third loop consists of the second sub-PM and the simple chain III, namely, $loop_3$\{-$R_{45}||R_{44}\perp R_{43}||R_{42}||P_{41}$-\}, we have

$$\xi_{L3} = \dim\left\{\begin{bmatrix} t^3 \\ r^1(\| R_{35}) \end{bmatrix} \cup \begin{bmatrix} t^3 \\ r^2(\| \lozenge(R_{42}, R_{44}) \end{bmatrix}\right\} = \dim\left\{\begin{bmatrix} t^3 \\ r^2(\| \lozenge(R_{42}, R_{44}) \end{bmatrix}\right\} = 5$$

Similarly, the DOF of the third loop is obtained from Eq. (5), F_1=5-5=0

Thus, the number of DOF for the PM can be determined by Eq. (4) as follows.

$$F=F_1+F_2+F_3=3+1+0=4$$

Through strategic actuation of prismatic joints P_{11}~P_{41} on the base platform 0, the moving platform 1 achieves 3T combined with rotational motion about the R_{15} axis, thereby fully realizing its 3T1R kinematic potential.

Furthermore, X-axis displacement is exclusively controlled by prismatic joint P_{21}. Y-axis displacement is solely governed by prismatic joint P_{11}. Z-axis translation and platform attitude angles require coordinated actuation of all four prismatic joints (P_{11}~P_{41}). Therefore this PM exhibits enhanced partial motion decoupling properties, demonstrating significant advantages in precision trajectory planning applications.

3 Position Analysis

The kinematic model of the PM is illustrated in Fig. 2. The base platform 0 is defined as a rectangular frame with length $2a$ along the X-axis and width $2c$ along the Y-axis. The moving platform 1, depicted as an isosceles right triangle, features a waist length of b (*i.e.*, the length of each equal side). Let

$$E_2E_3=E_2E_4=b,\ A_iB_i=l_1(i=1,2,3,4),\ B_1C_1=B_2C_2=l_2,\ B_iC_i=l_3\ (i=3,4),$$
$$C_1D_1=C_2D_2=l_4,\ D_1D_2=2l_5,\ E_1E_2=l_6,\ C_iD_i=l_7\ (i=3,4),\ D_3E_3=D_4E_4=l_8.$$

A Cartesian base coordinate system O-XYZ is established with its origin at the center O of the base platform. Point F represents the geometric center of the moving platform 1, while point E_2 serves as the origin of the moving coordinate system. The axes (x', y', z') of this moving coordinate system are each parallel to their corresponding axes in the base system O-XYZ.

The attitude angle β, defined as the rotational displacement of platform 1 about the Z-axis, is represented by the counter clockwise rotation of FE_2 around an axis parallel to the Z-axis (see Fig. 2b). In the second loop, the intermediate variable α is designated as the positive angle between segment B_3C_3 and the X-axis. Similarly, in the third loop, α_0 is established as the positive angle formed between segment B_4C_4 and the X-axis direction.

3.1 Forward Position

The forward position solution involves determining the 3T coordinates (x, y, z) of point O' and the orientation angle β of the moving platform, given the known coordinates of four reference points A_1-A_4, specifically y_1, x_2, y_3, x_4, on the base platform.

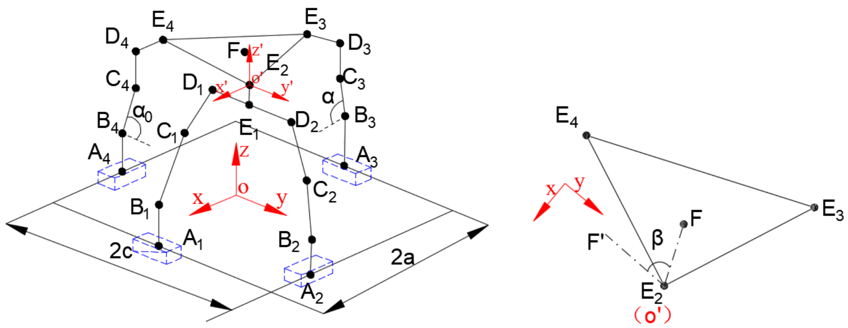

(a) Kinematic model (b) Projection on *xoy* plane

Fig. 2 Kinematic model of the 3T1R PM

Let the Z-axis position of the reference point, denoted as z*, the virtual Z-coordinate of the base point, be defined as an auxiliary variable. Following the topological characteristics-based kinematic methodology for robotic mechanisms[5], the symbolic kinematics of the PM can be derived through the following procedure.

1) In the first loop, it is easily obtained below.

$$A_2=(x_2,\ c,\ 0),\ B_2=(x_2,\ c,\ l_1);\ A_1=(a,\ y_1,\ 0),\ B_1=(a,\ y_1,\ l_1)$$

$$E_1=(x,\ y,\ z^*-l_6),\ D_1=(x,\ y-l_5,\ z^*-l_6),\ D_2=(x,\ y+l_5,\ z^*-l_6)\ .$$

$$x = x_2 \tag{7}$$

$$y = y_1 + l_5 \tag{8}$$

$$z^* = l_1 + l_3 sin\alpha + l_7 \tag{9}$$

2) In the second loop, since the positive included angle between B_3C_3 and X axis is the intermediate variable α, i.e.,

$$A_3=(-a,\ y_3,\ 0),\ B_3=(-a,\ y_3,\ l_1),\ C_3=(-a+l_3\cos\alpha,\ y_3,\ l_1+l_3\sin\alpha),$$

$$D_3=(-a+l_3\cos\alpha,\ y_3,\ l_1+l_3\sin\alpha+l_7),\ E_3=(x-b\cos(\beta-\frac{\pi}{4}),\ y+b\sin(\beta-\frac{\pi}{4}),\ z^*),$$

According to the link length $D_3E_3=l_8$, we can get

$$[x-bcos(\beta-\frac{\pi}{4})+a-l_3cos\alpha]^2+[y+bsin(\beta-\frac{\pi}{4})-y_3]^2=l_8^{\ 2} \tag{10}$$

3) In the third loop, we take the same link lengths since SOC$_{II}$ and SOC$_{III}$ are the same topology, *i.e.*, $A_iB_i=l_1$, $B_iC_i=l_3$ and $C_iD_i=l_7(i=3,4)$, which lead to $\alpha_0=\alpha$. Further, there are the following equations.

$$A_4=(x_4,\ -c,\ 0),\quad B_4=(x_4,\ -c,\ l_1),\quad C_4=(x_4,\ -c+l_3\cos\alpha,\ l_1+l_3\sin\alpha),$$

$$D_4=(x_4,\ -c+l_3\cos\alpha,\ l_1+l_3\sin\alpha+l_7),\quad E_4=(x-b\sin(\beta-\frac{\pi}{4}),\ y-b\cos(\beta-\frac{\pi}{4}),\ z^*)$$

By the constraint of link length $D_4E_4=l_8$, there are

$$[x-bsin(\beta-\frac{\pi}{4})-x_4]^2+[y-bcos(\beta-\frac{\pi}{4})+c-l_3cos\alpha]^2=l_8^2 \tag{11}$$

So far, from Eqs. (10) and (11), we can get below

$$\alpha=\arccos\left(\frac{E-b\cos\left(\beta-\frac{\pi}{4}\right)+p\sqrt{l_8^2-\left(F+b\sin\left(\beta-\frac{\pi}{4}\right)\right)^2}}{l_3}\right) \tag{12}$$

where $p=\pm1$, $E=a+x$, $F=y-y_3$

$$\beta=q\pi+\frac{\pi}{4}+m\arcsin\left\{\frac{(E-c)^2+(x-x_4)^2+y^2-2Ey-F^2+2cy}{2b(F+x-x_4)}+n\frac{(c-E+y)}{b}\right.$$
$$\left.+\left\{\frac{E-c-y}{2}+\sqrt{\frac{(F+x-x_4)^2\left[4l_8^2-2cy+2Fx_4-y^2+2Ey-F^2-2Fx-(E-c)^2-(x-x_4)^2\right]}{4\left[(E-c)^2+(x-x_4)^2+y^2-2Ey+F^2+2Fx-2Fx_4+2cy\right]}}\right\}\right\} \tag{13}$$

where, $q=0$ or 1, $m=\pm1$, $n=\pm1$.

The orientation angle β is directly computed from Eq. (13). The following substitution of β into Eq. (12) yields parameter α, which in turn enables determination of the vertical coordinate z through the kinematic relationship.

The analysis reveals eight distinct forward kinematic solution sets. This multiplicity originates from the quadratic solution space of parameter α (yielding two valid configurations), with each α solution branch subsequently generating four feasible orientation angle β variants through trigonometric resolution.

3.2 Inverse Position

The inverse kinematics of the PM require determining the actuator coordinates (y_1, x_2, y_3, x_4) for the base platform points A_1-A_4, given the prescribed 3T coordinates (x, y, z) of reference point O' and the orientation angle β of the moving platform. This inverse mapping can be resolved through *Eqs.*(10)~(11), which govern the following derivations.

$$y_1=y-l_5 \tag{14}$$

$$x_2 = x \tag{15}$$

From Eqs. (10) and (11), we can get

$$y_3 = y + b\sin(\beta - \frac{\pi}{4}) + u\sqrt{l_8{}^2 - \left[x - b\cos(\beta - \frac{\pi}{4}) + a - l_3\cos\alpha\right]^2} \tag{16}$$

$$x_4 = x - b\sin(\beta - \frac{\pi}{4}) + w\sqrt{l_8{}^2 - \left[y - b\cos(\beta - \frac{\pi}{4}) + c - l_3\cos\alpha\right]^2} \tag{17}$$

Where u=±1 and w=±1.

Henceforth, there are four sets of solutions in total since the input values y_1 and x_2 have only one set of solutions, and y_3 and x_4 have two sets of solutions.

The above formula has been verified to be consistent with Adams simulation.

4 Singularity Analysis

The input and out Jacobian matrix J_i, J_o can be derived through inverse kinematics analysis of the PM[6, 7], respectively, based on which we have the following observations.

When det(J_i)=0, that is, g_{33}=0 or g_{44}=0, or both are 0, the PM produces input singularity. There are three situations below.

when y_3=y_{E3}, the configuration is shown in Fig. 3(a).

when x_4=x_{E4}, the configuration is shown in Fig. 3(b).

when y_3=y_{E3} and x_4=x_{E4}, the configuration is shown in Fig. 3(c).

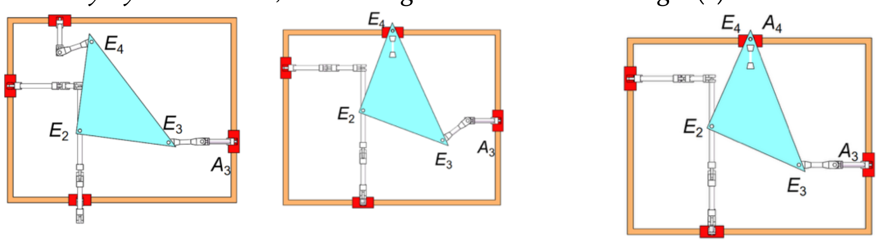

(a) Input singular position 1 (b) Input singular position 2 (c) Input singular position 3

Fig. 3 Input singular positions of the 3T1R PM

(2) When det(J_o)=0, that is, $f_{34}f_{43}$=0, the PM produces output singularity as follows.

F_{34}=0, namely

$$\sin\left(\beta-\frac{\pi}{4}\right)\left[x_{D_3}-x_{E_3}\right]=\cos\left(\beta-\frac{\pi}{4}\right)\left[y_{E_3}-y_3\right]$$

f_{43}=0, At this time, there are two situations, namely,

① α=0°, the configuration is shown in Fig. 4(a).

② $y_{D3}=y_{E3}$, the configuration is shown in Fig. 4(b).

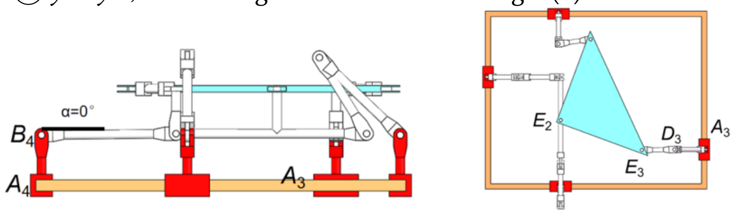

(a) Output singular position 1 (b) Output singular position 2

Fig.4 Output singular positions of the 3T1R PM

(3) When det(J_i)=det(J_o)=0, the PM produces comprehensive singularity. At this time, there is only one case, i.e, $y_{D3}=y_{E3}$.

The workspace calculation based on the forward solutions, and the dynamic modeling and analysis of the PM have been carried out[7], which are omitted here due to the space the paper.

5 Conclusions

In this work, a novel topology for a 4-DOF 3T1R PM is presented. The symbolic solutions for both forward and inverse position, and singularity of the PM are analytically derived, revealing inherent partial motion decoupling characteristics, which are not possessed by 4-DOF H4, I4, and Par4 PMs. The 3T1R PM can be used in industrial object grasping, sorting materials, adjusting workpiece attitude, etc.

Acknowledgment The financial support from the National Natural Science Foundation of China (NSFC No. 52375007) is acknowledged.

References

1.Nabat V, Rodriguez M D L O, Company O, Krut S, Pierrot F (2005) Par4: very high speed parallel robot for pick-and-place. Proceedings of the IEEE/RSJ International Conference on Intelligent Robots and Systems 1202-1207.

2.Kong X. and Gosselin C.M.. Type synthesis of 3T1R 4-DOF parallel manipulator based on screw theory. IEEE Transactions on Robotics and Automation, 20(2):181-190, 2004

3.Yang Tingli, Liu Anxin, Shen Huiping, et.al, Topology design of robot mechanism. Singapore: Springer (2018).

4.Shen Huiping, Li Ju, Wu Guanglei, Deng Jiaming, Topological Structure Optimization for Parallel Robotic Mechanisms, Beijing: Higher Education Press (2025).

5. Shen Huiping, Topological Characteristics-Based Kinematics for Robot Mechanisms. Beijing: Higher Education Press(2021).

6. Bao Shaoping, Wu Guanglei, Design analysis and dynamic modeling of a high-speed 3T1R parallel robot for pick-and-place application. International Journal of Mechanisms and Robotic Systems, 3(2/3), 237-237(2016).

7. Fu Zeng, Topology design and performance analysis of novel 3-DOF and 4-DOF parallel mechanisms, Changzhou University, 2025.